Noname manuscript No.
(will be inserted by the editor)

Free Convection in a Brinkman-Darcy Flow of Solutal Stratified Micropolar Fluid under Radiation Boundary Conditions

Upendar Mendu · D. Srinivasacharya · Saeid Abbasbandy · Ali J Chamkha

Received: date / Accepted: date

Abstract This work deals with Lie group analysis of free convection about a vertical plate subjected to mixed thermal boundary conditions in a Brinkman-Darcy flow of solutal stratified micropolar fluid. The governing boundary layer equations are cast into coupled nonlinear ordinary differential equations using the Lie Group point transformations. These transformed governing equations and the transformed thermal boundary condition on the surface of the plate involve in a non-negative parameter m, which assumes the values $0, 1$ and ∞ for the cases of prescribed temperature, prescribed heat flux and radiation boundary condition. These governing equations of the physics has been solved using the Homotopy Analysis Method (HAM). To discuss the salient features of the radiation boundary condition on the fluid flow, the boundary layer velocity, microrotation, temperature and concentration profiles were plotted under the radiation boundary condition for the effect of coupling number, Darcy's number and solutal stratification coefficient.

Keywords Lie Group Analysis · Solutal Stratification · Free Convection · Micropolar Fluid · Mixed Thermal Boundary Condition

1 Introduction

[1] has pioneered the problem of the convective heat transfer from a heated vertical plate. Later a great deal of attention has been drew by many researchers on the problem of free convection next to heated vertical surface. These earlier studies of the free-convection boundary-layer flow over a heated surface have dealt with numerical solutions associated with either prescribed surface temperature or heat flux. The problem of free convection has not received enough attention when the plate subjected to a radiation boundary condition (RBC) or when it is subject to a mixed thermal boundary condition. [2] has studied a similarity analysis of free convection about a wedge and a cone which are subjected to mixed thermal boundary conditions. A similarity analysis was performed by [3] to investigate the laminar free-convection boundary-layer flow in the presence of a transverse magnetic field over a wedge with mixed thermal boundary conditions. [4] studied the steady natural convection boundary layer flow over a downward pointing vertical cone in porous media saturated with non-Newtonian power-law fluids under mixed thermal boundary conditions. Recently [5] analyzed a similarity solution of the steady free convection boundary layer over vertical and horizontal surfaces embedded in a fluid-saturated porous medium with mixed thermal boundary conditions. The aim of the present study is to obtain similarity solutions for the velocity, microrotation, temperature and concentration profiles under the mixed thermal boundary conditions.

Extensive studies of free convection heat and mass transfer of a non-isothermal vertical surface under boundary layer approximation have been undertaken by several authors. A detailed coverage of research works related to convective heat transfer and the variant applications are reviewed in recent books by [6–8]. The majority of these studies dealt with the traditional Newtonian fluids. It is well known that most of the fluids which are encountered in chemical and allied processing applications do not satisfy the classical Newton's law and are accordingly known as non-Newtonian fluids. Due to the salient applications of non-Newtonian fluids

Upendar Mendu
Department of Mathematics
GITAM University, Hyderabad - 502 329
E-mail: upendarmendu@gmail.com

in biology, physiology, technology, and industry, considerable efforts have been directed towards the analysis and understanding of such fluids. A number of mathematical models have been proposed to explain the rheological behavior of non-Newtonian fluids. Among these, the fluid model introduced by [9], exhibits some microscopic effects arising from the local structure and micro motion of the fluid elements. Further, they can sustain couple stresses and include classical Newtonian fluid as a special case. The model of micropolar fluid represents fluids consisting of rigid, randomly oriented (or spherical) particles suspended in a viscous medium where the deformation of the particles is ignored. Micropolar fluids have been shown to accurately simulate the flow characteristics of polymeric additives, geomorphologic sediments, colloidal suspensions, haematological suspensions, liquid crystals, lubricants etc. The mathematical theory of equations of micropolar fluids and applications of these fluids in the theory of lubrication and in the theory of porous media are presented by [10]. Free convection of heat and mass transfer in non-Newtonian fluid have great importance in engineering applications; for instance, the thermal design of industrial equipment dealing with molten plastics, polymeric liquids, foodstuffs, or slurries. Several investigators have extended many of the available convection heat and mass transfer problems to include the non-Newtonian effects.

During the last several decades due to its great practical applications in modern industry, the heat and mass transfer in fluid-porous media has received a growing interest. The utilization of thermal energy, design of building components for energy consideration, control of pollutant spread in groundwater, compact heat exchangers, solar power collectors and food industries, to name just a few applications. An excellent review of existing theoretical and experimental work on this subject can be found in the recent books and monographs by [11–16].

In order to treat the encountered nonlinear partial differential equations in engineering and science few methods are available. Very often the only way to provide insight into qualitative and quantitative aspects of the solutions is to determine the physical symmetries of all the given nonlinear partial differential equations through the group analysis [17–19]. For the system of partial differential equations we determine the infinitesimal generators X in one parameter admitted by them. The Lie group of point transformations reduce the independent variables than in the given system of PDE's and transforms the independent variables into a single independent variable, called the similarity variable, to get similarity (invariant) solutions for the invariant geometries without alter the structural form of the given system of equations under investigation. This method has drew the attention of several researchers [20–26].

2 MATHEMATICAL FORMULATION

Consider a steady, laminar, incompressible, two-dimensional free convective heat and mass transfer along a semi infinite vertical plate embedded in a solutal stratified non-Darcy micropolar fluid. Choose the co-ordinate system such that $\overline{x}$ axis is along the vertical plate and $\overline{y}$ axis normal to the plate. The plate is maintained with the mixed thermal boundary condition and variable wall concentration $\overline{C}_w(\overline{x})$. The mass concentration of the ambient medium is assumed to be linearly stratified in the form $\overline{C}_\infty(\overline{x}) = C_{\infty,0} + B_1\overline{x}$, where B_1 is constant and varied to alter the intensity of stratification in the medium, T_∞ is the ambient temperature and $C_{\infty,0}$ is the beginning ambient concentration at $\overline{x} = 0$, respectively.

By employing laminar boundary layer flow assumptions, Boussinesq approximation, using the Darcy-Brinkman model and Dupuit- Forchheimer relationship ([12]), the governing equations for the micropolar fluid are given by:

$$\frac{\partial \overline{u}}{\partial \overline{x}} + \frac{\partial \overline{v}}{\partial \overline{y}} = 0 \tag{1}$$

$$\left.\begin{aligned} &\frac{1}{{\epsilon_p}^2}\left(\overline{u}\frac{\partial \overline{u}}{\partial \overline{x}} + \overline{v}\frac{\partial \overline{u}}{\partial \overline{y}}\right) = \frac{\mu+\kappa}{\epsilon_p\,\rho}\frac{\partial^2 \overline{u}}{\partial \overline{y}^2} + \frac{\kappa}{\rho}\frac{\partial \overline{\omega}}{\partial \overline{y}} - \\ &\frac{\mu}{\rho\,K_p}\overline{u} + g^*\left(\beta_T(\overline{T}-T_\infty) + \beta_C(\overline{C}-C_\infty)\right) \end{aligned}\right\} \tag{2}$$

$$\frac{1}{\epsilon_p}\left(\overline{u}\frac{\partial \overline{\omega}}{\partial \overline{x}} + \overline{v}\frac{\partial \overline{\omega}}{\partial \overline{y}}\right) = \frac{\gamma}{\rho j}\frac{\partial^2 \overline{\omega}}{\partial \overline{y}^2} - \frac{\kappa}{\rho j}\left(2\overline{\omega} + \frac{1}{\epsilon_p}\frac{\partial \overline{u}}{\partial \overline{y}}\right) \tag{3}$$

$$\overline{u}\frac{\partial \overline{T}}{\partial \overline{x}} + \overline{v}\frac{\partial \overline{T}}{\partial \overline{y}} = \alpha\frac{\partial^2 \overline{T}}{\partial \overline{y}^2} \tag{4}$$

$$\overline{u}\frac{\partial \overline{C}}{\partial \overline{x}} + \overline{v}\frac{\partial \overline{C}}{\partial \overline{y}} = D\frac{\partial^2 \overline{C}}{\partial \overline{y}^2} \tag{5}$$

where $\overline{u}$ and $\overline{v}$ are the components of velocity along $\overline{x}$ and $\overline{y}$ directions respectively, $\overline{\omega}$ is the component of microrotation whose direction of rotation lies normal to the $\overline{xy}$-plane, g^* is the gravitational acceleration, $\overline{T}$ is the temperature, $\overline{C}$ is the concentration, β_T is the coefficient of thermal expansions, β_C is the coefficient of solutal expansions, μ is the dynamic coefficient of viscosity of the fluid, κ is the vortex viscosity, γ is the spin-gradient viscosity, σ is the magnetic permeability of the fluid, ν is the kinematic viscosity, α is the thermal diffusivity, D is the molecular diffusivity. We follow the work of many recent authors by assuming that $\gamma = (\mu+\kappa/2)j$. This assumption is invoked to allow the field of equations predicts the correct behavior in the limiting case when the microstructure effects become negligible and the total spin ω reduces to the angular velocity.

The boundary conditions are:

$$\overline{u} = 0,\, \overline{v} = 0,\, \overline{\omega} = 0,\, \overline{C} = \overline{C}_w(\overline{x}) \quad \text{at} \quad \overline{y} = 0 \tag{6}$$

$$\overline{u} \to 0,\, \overline{\omega} \to 0,\, \overline{T} \to T_\infty,\, \overline{C} \to C_\infty(\overline{x}) \text{as} \overline{y} \to \infty \tag{7}$$

The generalized form of the mixed thermal boundary condition on the surface of the vertical plate ($\overline{y} = 0$) is assumed as:

$$a_0(\overline{x})(\overline{T} - T_\infty)_{\overline{y}=0} - a_2(\overline{x})\left(\frac{\partial \overline{T}}{\partial \overline{y}}\right)_{\overline{y}=0} = a_2(\overline{x}) \tag{8}$$

where the subscripts w and ∞ indicates the conditions at wall and at the outer edge of the boundary layer, respectively. The boundary condition $\omega = 0$ in Eq. 6 at wall, i.e., at $\overline{y} = 0$, represents the case of concentrated particle flows in which the micro elements close to the wall are not able to rotate, due to the no - slip condition.

3 METHOD OF SOLUTION

Introducing the following non-dimensional variables

$$\left.\begin{aligned}
& x = \frac{\overline{x}}{L}, \quad y = \frac{\overline{y}}{L} Gr^{\frac{1}{4}}, \quad u = \frac{\overline{u}\, L}{\nu\, Gr^{\frac{1}{2}}}, v = \frac{\overline{v}\, L}{\nu\, Gr^{\frac{1}{4}}}, \\
& \omega = \frac{\overline{\omega}\, L^2}{\nu\, Gr^{\frac{3}{4}}}, Gr = \frac{g^* \beta_T \Delta T L^3}{\nu^2}, \theta = \frac{\overline{T} - \overline{T}_\infty}{\overline{T}_w(\overline{x}) - T_\infty}, x \\
& \Delta T = \overline{T}_w(\overline{x}) - T_\infty, \phi = \frac{\overline{C} - \overline{C}_\infty(\overline{x})}{\overline{C}_w(\overline{x}) - C_\infty}, \\
& x\, \Delta C = \overline{C}_w(\overline{x}) - C_\infty
\end{aligned}\right\} \tag{9}$$

and the stream function ψ through $u = \frac{\partial \psi}{\partial y}$ and $v = -\frac{\partial \psi}{\partial x}$ in to the Eqs. (1) - (5) and (6) - (8) we get

$$\left.\begin{aligned}
& \frac{1}{\epsilon_p^2}\left(\frac{\partial \psi}{\partial y}\frac{\partial^2 \psi}{\partial x \partial y} - \frac{\partial \psi}{\partial x}\frac{\partial^2 \psi}{\partial y^2}\right) = \left(\frac{1+K}{\epsilon_p}\right)\frac{\partial^3 \psi}{\partial y^3} + \\
& K\,\frac{\partial \omega}{\partial y} + x[\theta + B\phi] - \left(\frac{1}{D_a}\right)\frac{\partial \psi}{\partial y}
\end{aligned}\right\} \tag{10}$$

$$\left.\begin{aligned}
& \frac{1}{\epsilon_p}\left(\frac{\partial \psi}{\partial y}\frac{\partial \omega}{\partial x} - \frac{\partial \psi}{\partial x}\frac{\partial \omega}{\partial y}\right) = \left(1 + \frac{K}{2}\right)\frac{\partial^2 \omega}{\partial y^2} - \\
& K\left(2\omega + \frac{1}{\epsilon_p}\frac{\partial^2 \psi}{\partial y^2}\right)
\end{aligned}\right\} \tag{11}$$

$$x\frac{\partial \psi}{\partial y}\frac{\partial \theta}{\partial x} - x\frac{\partial \psi}{\partial x}\frac{\partial \theta}{\partial y} + \frac{\partial \psi}{\partial y}\theta = \frac{1}{Pr}x\frac{\partial^2 \theta}{\partial y^2} \tag{12}$$

$$x\frac{\partial \psi}{\partial y}\frac{\partial \phi}{\partial x} - x\frac{\partial \psi}{\partial x}\frac{\partial \phi}{\partial y} + \frac{\partial \psi}{\partial y}\phi + \epsilon_2\frac{\partial \psi}{\partial y} = \frac{1}{Sc}x\frac{\partial^2 \phi}{\partial y^2} \tag{13}$$

where $K = \frac{\kappa}{\mu}$ is the Coupling number, $B = \frac{\beta_c\, \Delta C}{\beta_T\, \Delta T}$ is the buoyancy parameter, $Da = \frac{K_p}{L^2} Gr^{1/2}$ is the Darcy number, $Pr = \frac{\nu}{\alpha}$ is the Prandtl number and $Sc = \frac{\nu}{D}$ is the Schmidth number.

The transformed boundary conditions are

$$\left.\begin{aligned}
& \frac{\partial \psi}{\partial y} = 0,\, \frac{\partial \psi}{\partial x} = 0,\, \omega = 0,\, \phi(x,0) = 1 - L\epsilon_2 \\
& b_0\, \Delta T\, \theta(x,0) - b_1\, (\Delta T)^{\frac{5}{4}}\, \theta'(x,0) = 1, \text{at} y = 0
\end{aligned}\right\} \tag{14}$$

$$\frac{\partial \psi}{\partial y} \to 0, \omega \to 0, \theta \to 0, \phi \to 0 \quad \text{as} \quad y \to \infty \tag{15}$$

The functions $b_0(x)$ and $b_1(x)$ of Eq.(14) are given by

$$b_0(x) = \frac{a_0(\overline{x})}{a_2(\overline{x})}x \text{ and } b_1(x) = \left(\frac{g^*\, \beta_T\, x^4}{L\, \nu^2}\right)^{\frac{1}{4}} \frac{a_1(\overline{x})}{a_2(\overline{x})}x$$

Each of these functions must be equal to a constant to enable a similarity solution and they are referred to as b_0 and b_1 hereon. For given values of the constants b_0, b_1 and T_∞, the reference temperature T may be chosen to satisfy the following equation without any loss of generality,

$$b_1\, (\Delta T)^{\frac{5}{4}} + b_0\, \Delta T - 1 = 0 \tag{16}$$

By defining $m = b_1\, (\Delta T)^{\frac{5}{4}}$, the thermal boundary condition can be written as

$$(1 - m)\, \theta(x,0) - m\theta'(x,0) = 1 \tag{17}$$

Similarity solutions via Lie group analysis

We now introduce the one-parameter scaling group of transformations which is a simplified form of Lie group transformation

$$\left.\begin{aligned}
& \Gamma: \quad \widehat{x} = xe^{\epsilon\alpha_1}, \widehat{y} = ye^{\epsilon\alpha_2}, \widehat{\psi} = \psi e^{\epsilon\alpha_3}, \widehat{\omega} = \omega e^{\epsilon\alpha_4}, \\
& \widehat{\theta} = \theta e^{\epsilon\alpha_5}, \widehat{\phi} = \phi e^{\epsilon\alpha_6}
\end{aligned}\right\} \tag{18}$$

where α_1, α_2, α_3, α_4, α_5, α_6 are transformation parameters and ϵ is a small parameter. This scaling group of transformations transform coordinates $(x,\, y,\, \psi,\, \omega,\, \theta,\, \phi)$ to $\left(\widehat{x},\, \widehat{y},\, \widehat{\psi},\, \widehat{\omega},\, \widehat{\theta},\, \widehat{\phi}\right)$. Equations (10) to (13) and boundary conditions (14) are invariant under the point transformations (18).

In view of the transformations (18), Eqs. (10) - (13) become

$$\left.\begin{array}{l}\dfrac{e^{\epsilon(\alpha_1+2\alpha_2-2\alpha_3)}}{{\epsilon_P}^2}\left(\dfrac{\partial\widehat{\psi}}{\partial\widehat{y}}\dfrac{\partial^2\widehat{\psi}}{\partial\widehat{x}\partial\widehat{y}}\right)-\dfrac{\partial\widehat{\psi}}{\partial\widehat{x}}\dfrac{\partial^2\widehat{\psi}}{\partial\widehat{y}^2}=\\ \left(\dfrac{1+K}{\epsilon_p}\right)e^{\epsilon\,(3\alpha_2-\alpha_3)}\dfrac{\partial^3\widehat{\psi}}{\partial\widehat{y}^3}+K\,e^{\epsilon\,(\alpha_2-\alpha_4)}\dfrac{\partial\widehat{\omega}}{\partial\widehat{y}}+\\ \widehat{x}\left(e^{\epsilon\,(-\alpha_1-\alpha_5)}\widehat{\theta}+B\,e^{\epsilon(-\alpha_1-\alpha_6)}\widehat{\phi}\right)-\\ \dfrac{1}{Da}\left(e^{\epsilon\,(-\alpha_2-\alpha_3)}\dfrac{\partial\widehat{\psi}}{\partial\widehat{y}}\right)\end{array}\right\}\quad(19)$$

$$\left.\begin{array}{l}\dfrac{e^{\epsilon(\alpha_1+\alpha_2-\alpha_3-\alpha_4)}}{\epsilon_p}\left(\dfrac{\partial\widehat{\psi}}{\partial\widehat{y}}\dfrac{\partial\widehat{\omega}}{\partial\widehat{x}}-\dfrac{\partial\widehat{\psi}}{\partial\widehat{x}}\dfrac{\partial\widehat{\omega}}{\partial\widehat{y}}\right)=\\ \left(1+\dfrac{K}{2}\right)e^{\epsilon(2\alpha_2-\alpha_4)}\dfrac{\partial^2\widehat{\omega}}{\partial\widehat{y}^2}-\\ K\left(2e^{-\epsilon(\alpha_4)}\widehat{\omega}+\dfrac{e^{\epsilon(2\alpha_2-\alpha_3)}}{\epsilon_p}\dfrac{\partial^2\widehat{\psi}}{\partial\widehat{y}^2}\right)\end{array}\right\}\quad(20)$$

$$\left.\begin{array}{l}e^{\epsilon(\alpha_2-\alpha_3-\alpha_5)}\left(\widehat{x}\dfrac{\partial\widehat{\psi}}{\partial\widehat{y}}\dfrac{\partial\widehat{\theta}}{\partial\widehat{x}}-\widehat{x}\dfrac{\partial\widehat{\psi}}{\partial\widehat{x}}\dfrac{\partial\widehat{\theta}}{\partial\widehat{y}}+\widehat{\theta}\dfrac{\partial\widehat{\psi}}{\partial\widehat{y}}\right)=\\ \dfrac{1}{Pr}\widehat{x}e^{\epsilon(-\alpha_1+2\alpha_2-\alpha_5)}\dfrac{\partial^2\widehat{\theta}}{\partial\widehat{y}^2}\end{array}\right\}\quad(21)$$

$$\left.\begin{array}{l}e^{\epsilon(\alpha_2-\alpha_3-\alpha_6)}\left(\widehat{x}\dfrac{\partial\widehat{\psi}}{\partial\widehat{y}}\dfrac{\partial\widehat{\phi}}{\partial\widehat{x}}-\widehat{x}\dfrac{\partial\widehat{\psi}}{\partial\widehat{x}}\dfrac{\partial\widehat{\phi}}{\partial\widehat{y}}+\widehat{\phi}\dfrac{\partial\widehat{\psi}}{\partial\widehat{y}}\right)=\\ \dfrac{1}{Sc}\widehat{x}e^{\epsilon(-\alpha_1+2\alpha_2-\alpha_6)}\dfrac{\partial^2\widehat{\phi}}{\partial\widehat{y}^2}\end{array}\right\}\quad(22)$$

and the associated boundary conditions become

$$\left.\begin{array}{l}\dfrac{\partial\widehat{\psi}}{\partial\widehat{y}}=0,\ \dfrac{\partial\widehat{\psi}}{\partial\widehat{x}}=0,\ \widehat{\omega}=0,\ \widehat{\phi}e^{-\epsilon\alpha_6}=1\text{at}\,\widehat{y}e^{-\alpha_2}=0\\ \dfrac{\partial\widehat{\psi}}{\partial\widehat{y}}\to 0,\ \widehat{w}\to 0,\ \widehat{\theta}\to 0,\ \widehat{\phi}\to 0\text{as},\widehat{y}e^{-\alpha_2}\to\infty\end{array}\right\}(23)$$

and the mixed thermal boundary condition reduces to

$$(1-m)\,e^{-\epsilon\,\alpha_5}\widehat{\theta}-me^{\epsilon(\alpha_2-\alpha_5)}\widehat{\theta}'=1 \quad (24)$$

Since the group transformations (18) keeps the system invariant, hence the relations among the parameters from the Equations (19) - (22) is as below

$$\left.\begin{array}{l}\alpha_1+2\alpha_2-2\alpha_3=-\alpha_1=3\alpha_2-\alpha_3=\alpha_2-\alpha_4=\\ -\alpha_1-\alpha_5=-\alpha_1-\alpha_6=\alpha_2-\alpha_3,\\ \alpha_1+\alpha_2-\alpha_3-\alpha_4=2\alpha_2-\alpha_4=-\alpha_4=2\alpha_2-\alpha_3,\\ \alpha_2-\alpha_3=\alpha_2-\alpha_3-\alpha_5=-\alpha_1+2\alpha_2-\alpha_5,\\ \alpha_2-\alpha_3=\alpha_2-\alpha_3-\alpha_6=-\alpha_1+2\alpha_2-\alpha_6\end{array}\right\}(25)$$

These relations give

$$\alpha_1=\alpha_3=\alpha_4 \quad \& \quad \alpha_2=0=\alpha_5=\alpha_6 \quad (26)$$

so the infinitesimal transformations reduces to point transformations in one parameter as follows

$$\left.\begin{array}{l}\Gamma:\widehat{x}=xe^{\epsilon\alpha_1},\widehat{y}=y,\widehat{\psi}=\psi e^{\epsilon\alpha_1},\\ \widehat{\omega}=\omega e^{\epsilon\alpha_1},\widehat{\theta}=\theta,\quad\widehat{\phi}=\phi.\end{array}\right\}\quad(27)$$

After expanding the Lie group of point transformations in one parameter using the Taylor's series in powers of ϵ by considering the terms up to $\mathbf{O}(\epsilon)$, we get

$$\left.\begin{array}{l}\widehat{x}-x=x\,\epsilon\,\alpha_1,\widehat{y}-y=0,\widehat{\psi}-\psi=\psi\,\epsilon\,\alpha_1,\\ \widehat{\omega}-\omega=\omega\,\epsilon\,\alpha_1,\widehat{\theta}-\theta=0,\widehat{\phi}-\phi=0.\end{array}\right\}\quad(28)$$

The corresponding characteristic equations are given by

$$\frac{dx}{x\alpha_1}=\frac{dy}{0}=\frac{d\psi}{\psi\alpha_1}=\frac{d\omega}{\omega\alpha_1}=\frac{d\theta}{0}=\frac{d\phi}{0}. \quad (29)$$

The self similar solutions of characteristic equations (29) give the similarity transformations as below

$$\left.\begin{array}{l}\widehat{y}=\eta,\quad\widehat{\psi}=\widehat{x}f(\eta),\quad\widehat{\omega}=\widehat{x}g(\eta),\\ \widehat{\theta}=\theta(\eta),\quad\widehat{\phi}=\phi(\eta).\end{array}\right\}\quad(30)$$

Substituting the Eq. (30) into Eqs. (19) - (22), we get

$$\left.\begin{array}{l}\dfrac{1+K}{\epsilon_p}\,f'''-\dfrac{1}{\epsilon_p^2}(f')^2+\dfrac{1}{\epsilon_p^2}ff''+Kg,+\theta+B\phi-\\ \left(\frac{1}{D_a}\right)f'=0,\end{array}\right\}(31)$$

$$\left.\begin{array}{l}\left(1+\frac{K}{2}\right)g''+\frac{1}{\epsilon_p}f\,g'-\frac{1}{\epsilon_p}f'\,g-\\ K\left(2g+\frac{1}{\epsilon_p}f''\right)=0,\end{array}\right\}\quad(32)$$

$$\frac{1}{Pr}\,\theta''-f'\,\theta+f\,\theta'=0, \quad (33)$$

$$\frac{1}{Sc}\,\phi''-f'\,\phi+f\,\phi'-\varepsilon_2\,f'=0. \quad (34)$$

The boundary conditions (14) in terms of f, g, θ and ϕ now get transformed into

$$\left.\begin{array}{lll}f'=0,f=0,g=0,\phi=1-\epsilon_2 & \text{at} & \eta=0\\ f'\to 0,g\to 0,\theta\to 0,\phi\to 0 & \text{as} & \eta\to\infty:\end{array}\right\}(35)$$

and the mixed thermal condition at $\eta = 0$ is given by

$$(1-m)\theta(0) - m\theta'(0) = 1 \tag{36}$$

The following cases of mixed thermal boundary condition are of special interest:

Case(a): Variable Wall Temperature(VWT):

If $T = T_w(x)$ on the wall (i.e., y = 0), where $T_w(x) = T_\infty + M_1\, x^m$ gives $m = 0$ thus mixed thermal boundary condition reduces to the form

$$\theta(0) = 1. \tag{37}$$

Case(b): Variable Wall Heat Flux(VWHF/VWMF):

In the case of variable wall heat flux case, if the thermal boundary condition on the wall is $-\dfrac{\partial T}{\partial y} = M_1\, x^m$, then this gives $m = 1$, hence, the mixed thermal boundary condition reduces to

$$\theta'(0) = -1. \tag{38}$$

Case(c): Radiation Boundary Condition (RBC):

At the wall i.e., at $y = 0$, radiative boundary condition $-\dfrac{\partial T}{\partial y} = M_1\, x^m (T_w(x) - T_\infty)$ gives $m \to \infty$, hence the mixed thermal boundary condition reduces to

$$\theta(0) + \theta'(0) = 0. \tag{39}$$

4 Skin-Friction and Wall Couple Stress

The non-dimensional skin friction C_f and wall couple stress M_w are given by

$$\left.\begin{aligned} C_f \frac{Re^2}{Gr^{\frac{3}{4}}} &= 2\,(1+K)\, f''(0) \quad \text{and} \\ M_w\, \frac{Re^2}{Gr} &= \left(1 + \frac{K}{2}\right) g'(0). \end{aligned}\right\} \tag{40}$$

5 Results and Discussion

The non-linear nonhomogeneous differential equations (31)-(34) are solved analytically under the boundary conditions (35) for the case (c) using HAM-based Mathematica package BVPh 2.0, [27]. This Mathematica package for nonlinear boundary value/eigenvalue problems is developed, which is based on the HAM and is free

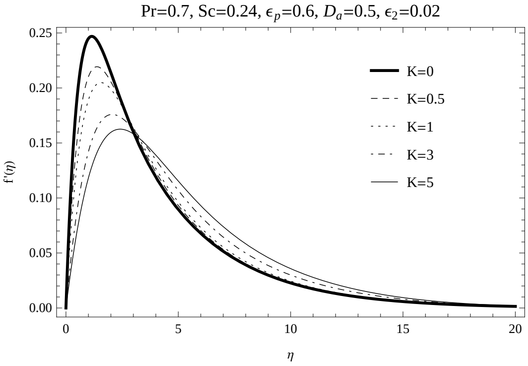

Fig. 1 Velocity profiles for various values of K

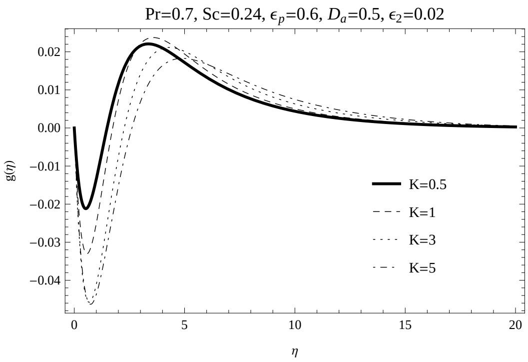

Fig. 2 Microrotation profiles for various values of K

available online. In the package BVPh, we should defined the linear auxiliary functions for Eqs. (31)-(34). These functions defined as

$$\left.\begin{aligned} &\mathcal{L}_1[f] = f''' - f',\ \mathcal{L}_2[g] = g'' - g, \\ &\mathcal{L}_3[\theta] = \theta'' - 4\theta,\ \mathcal{L}_4[\phi] = \phi'' - \phi. \end{aligned}\right\} \tag{41}$$

Also, we defined the initial approximations for the function solutions as

$$\left.\begin{aligned} &f_0(\eta) = 1 - 2e^{-\eta} + e^{-2\eta}, \quad g_0(\eta) = e^{-\eta} - e^{-2\eta}, \\ &\theta_0(\eta) = -\tfrac{e^{-3\eta}}{4} + e^{-\frac{3\eta}{4}}, \\ &\phi_0(\eta) = (1-\epsilon_2)(\tfrac{4e^{-\eta}}{3} - \tfrac{e^{-2\eta}}{3}). \end{aligned}\right\} \tag{42}$$

The accuracy of the high order approximation of the functions f, g, θ and ϕ are defined by the summation of averaged residual square of the governing equations (31)-(34).

For the case (c), i.e., radiation boundary condition (RBC) case, the Figs. 1 - 4 depict the variation of coupling number (K) on the profiles of velocity, microrotation, temperature and concentration with η. As for the consideration of the fluid model, the coupling number K characterized as a result of the coupling of linear and rotational motion arising from the micromotion

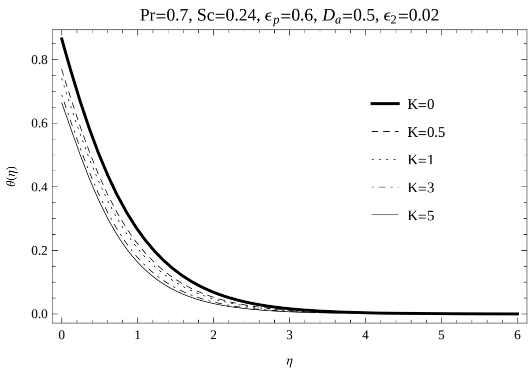

Fig. 3 Temperature profiles for various values of K

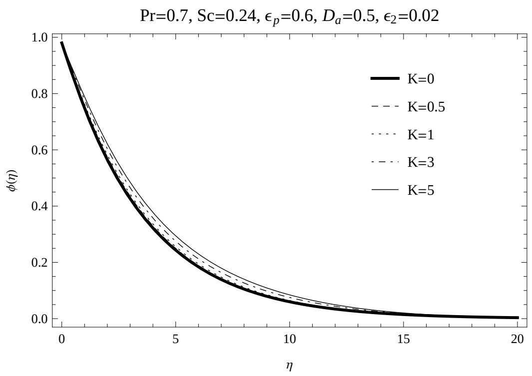

Fig. 4 Concentration profiles for various values of K

of the fluid molecules. Hence, $K = \dfrac{\kappa}{\mu}$ signifies the coupling between the Newtonian and rotational viscosities. The effect of microstructure becomes significant for the increasing values of K while the individuality of the substructure is much less pronounced for the decreasing values of K. We can see that in the limiting case of $K \to 0$, i.e., $\kappa \to 0$, the micropolarity of the fluid vanishes and the fluid behaves as nonpolar fluid, and this leads to the case of viscous fluid. It is observed from Fig.1 that the velocity decreases with the increase of K. The maximum of velocity decreases in amplitude and the location of the maximum velocity moves farther away from the wall with an increase of K. The velocity in case of micropolar fluid is less than that of the viscous fluid case ($K \to 0$ corresponds to viscous fluid). It is seen from Fig.2 that the microrotation component decreases near the vertical plate and increases far away from the plate with increasing coupling number K. The microrotation tends to zero as $K \to 0$ as is expected that in the limit $\kappa \to 0$ i.e. $K \to 0$ the Eqs. (1) and (2) are uncoupled with Eq. (3) and they reduce to viscous fluid flow equations. It is very interesting to notice from Fig. 3 that the temperature decreases with the increasing values of coupling number. It is clear from Fig. 4 that the non-dimensional concentration increases from

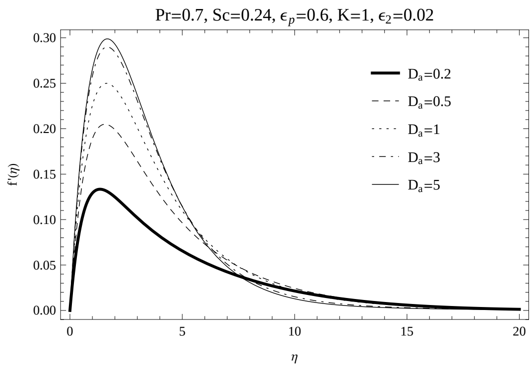

Fig. 5 Velocity profiles for various values of D_a

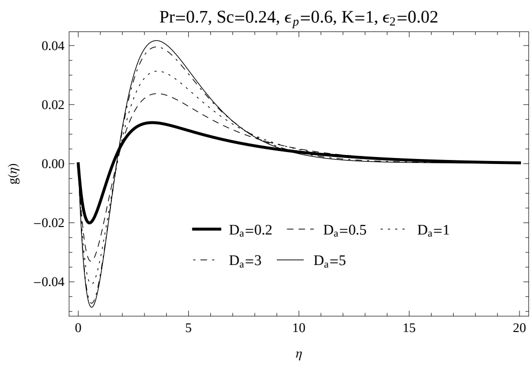

Fig. 6 Microrotation profiles for various values of D_a

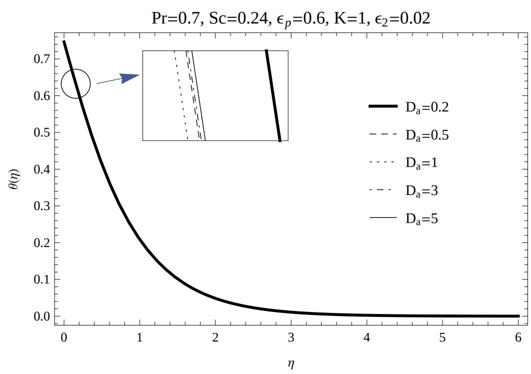

Fig. 7 Temperature profiles for various values of D_a

Newtonian case to non-Newtonian case (with increasing values of K).

The profiles of dimensionless velocity and microrotation for different values of Darcy number D_a are presented in Figs. 5 - 8 for the radiation boundary condition (RBC) case. Fig. 5 indicates that a rise in D_a (which implies a rise in permeability, K_p) enhances considerably the translational velocity of the micropolar fluid. Hence the micropolar fluid is decelerated with a rise in D_a. With increasing permeability the porous matrix structure becomes less prominent and in the limit of $D_a \to \infty$, the porous medium vanishes. This results in reduction of the velocity profile. Equation (2) shows

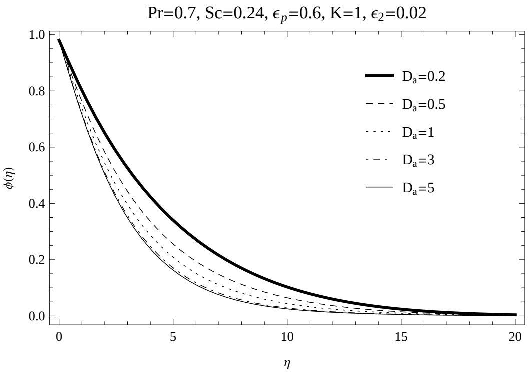

Fig. 8 Concentration profiles for various values of D_a

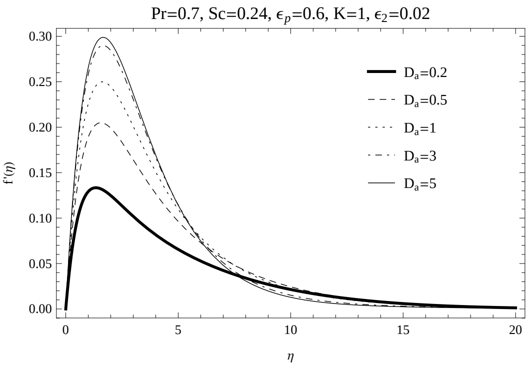

Fig. 9 Velocity profiles for various values of ε_2

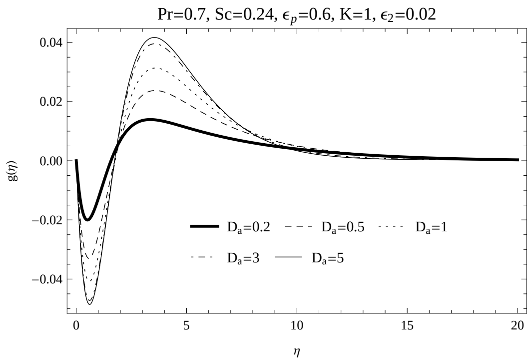

Fig. 10 Microrotation profiles for various values of ε_2

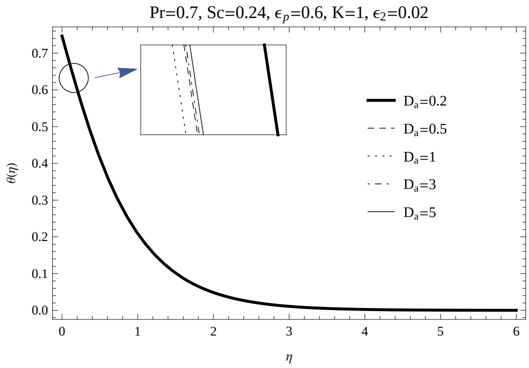

Fig. 11 Temperature profiles for various values of ε_2

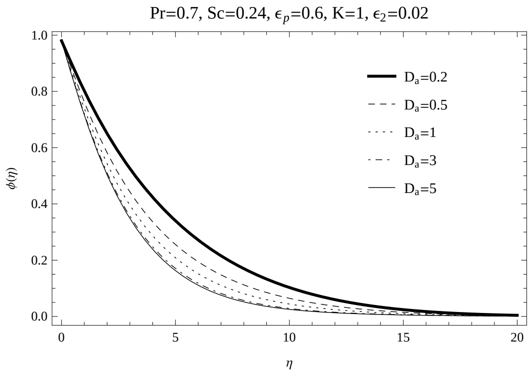

Fig. 12 Concentration profiles for various values of ε_2

that the Darcian body force is inversely proportional to D_a. Therefore higher D_a values will reduce the porous bulk retarding force (i.e., resistance force due to high solid material). The numerical computations also indicate that the presence of a porous medium with low permeability (i.e., high solid material presence) may be implemented successfully as a mechanism for controlling flow velocities in chemical engineering applications since lower permeability media induces a deceleration in transport. From Fig. 6, it can be observed that the microrotation decreases as D_a increases. The effect of D_a on temperature and concentration profiles can be seen in the Figs. 7 and 8. As D_a increases the temperature and concentration boundary layers were suppressed and compressed toward the surface. The dimensionless velocity component, microrotation,temperature and concentration for different values of solutal stratification parameter ε_2 are depicted in Figs. 9-12. From Fig. 9 it is observed that the velocity of the fluid decreases with the increase of solutal stratification parameter. From Fig. 10 we observe that the microrotation values change sign from negative to positive within the boundary layer. Also, it is clear that the magnitude of the microrotation increases with an increase in solutal stratification parameter. It is noticed from Fig. 11 the temperature of the fluid decreases with the increase of solutal stratification parameter. It is clear from Fig. 12 that the non-dimensional concentration of the fluid decreases with the increase of thermal stratification parameter.

References

1. E.M. Sparrow, J.L. Gregg, Laminar free convection from a vertical plate with uniform surface heat flux, Trans. ASME. **78**, 435 (1956)
2. G. Ramanaiah, G. Malarvizhi, Free convection about a wedge and a cone subjected to mixed thermal boundary conditions, Acta Mechanica. **93**, 119 (1992)

3. M.C. Ece, Free-convection flow about a wedge under mixed thermal boundary conditions and a magnetic field, Heat Mass Transfer. **41 (4)**, 291 (2005)
4. C.Y. Cheng, Natural convection heat transfer of non-newtonian fluids in porous media from a vertical cone under mixed thermal boundary conditions, Int. Commun. Heat Mass Transfer. **36**, 693 (2009)
5. R. Nazar, N.M. Arifin, I. Pop, Free convection boundary layer flow over vertical and horizontal flat plates embedded in a porous medium under mixed thermal boundary conditions, Int. Commun. Heat Mass Transfer. **33**, 87 (2006)
6. I. Pop, D. Ingham, *Analysis of Heat and Mass Transfer* (McGraw Hill, Newyark, 1972)
7. E. Eckeret, R. Drake, *Convective Heat Tranfer:Mathematical and Computational Modeling of Viscous Fluid and Porous Media* (Pergamon, Oxford, UK., 2001)
8. H. Schlichting, *Boundary-Layer Theory* (McGraw-Hill Book Co.,, 1979)
9. A.C. Eringen, Theory of micropolar fluids, J. Math. Mech. **16**, 1 (1966)
10. G. Lukaszewicz, *Micropolar FluidsTheory and Applications* (Birkhauser, Basel, 1999)
11. D.B. Ingham, I. Pop, *Transport Phenomena in Porous Media* (Pergamon, Oxford, 1998)
12. D.A. Nield, A. Bejan, *Convection in Porous Media* (Springer-Verlag, New York, 2006)
13. K. Vafai, *Handbook of Porous Media* (Marcel Dekker, New York, 2000)
14. I. Pop, D.B. Ingham, *Convective Heat Transfer : Mathematical and Computational Modelling of Viscous Fluids and Porous Media* (Pergamon, Oxford, 2001)
15. D.B. Ingham, A. Bejan, E. Mamut, I. Pop, *Emerging Technologies and Techniques in Porous Media* (Kluwer, Dordrecht, 2004)
16. A. Bejan, I. Dincer, S. Lorente, A.F. Miguel, A. Rei, *Porous and Complex Flow Structures in Modern Technologies* (Springer, New York, 2004)
17. A. Cohen, *An Introduction to the Lie Theory of One-Parameter of Groups:with Applications to the Solution of Differential Equations* (D. C. Heth & Co., 1911)
18. G.W. Bluman, S. Kumei, *Symmetries and Differential Equations* (Springer-Verlag, Newyark, Inc, 1989)
19. L. Ovsiannikov, *Group Analysis of Differential Equations* (Academic., 1982)
20. T. Hibiki, M. Ishii, Development of one-group interfacial area transport equation in bubbly flow systems, Int. J. Heat Mass Transfer. **45**, 2351 (2002)
21. M.A.A. Hamad, Analytical solution of natural convection flow of a nanofluid over a linearly stretching sheet in the presence of magnetic field, Int. Commun. Heat Mass Transfer. **38**, 487 (2011)
22. T. Tanthanuch, S.V. Meleshko, On definition of an admitted lie group for functional differential equations, Commun. Nonlinear Sci. Numer. Simul. **9**, 117 (2004)
23. F. Casas, Solution of linear partial differential equations by lie algebraic methods, J. Comput. Appl. Math. **76**, 159 (1996)
24. F.A. Salama, Lie group analysis for thermophoretic and radiative augmentation of heat and mass transfer in a brinkmandarcy flow over a flat surface with heat generation, Acta Mech. Sin. **27**, 159 (1996)
25. M.A.A. Hamad, I. Pop, Scaling transformations for boundary layer flow near the stagnation-point on a heated permeable stretching surface in a porous medium saturated with a nanofluid and heat generation/absorption effects, Transp. Porous Media. **87**, 25 (2011)
26. G. Bluman, P. Broadbridge, J.R. King, M.J. Ward, Similarity: generalizations, applications and open problems, J. Eng. Math. **66**, 1 (2010)
27. S.J. Liao, *Homotopy Analysis Method in Nonlinear Differential Equations* (Heidelberg & Beijing: Springer & Higher Education Press, 2012)